# Ground state quantum vortex proton model

Steven C. Verrall, Micah Atkins, Andrew Kaminsky, Emily Friederick, Andrew Otto,  $^{1, \, a)}$  Kelly S. Verrall,  $^2$  and Peter Lynch  $^3$ 

<sup>1)</sup>Physics Department, University of Wisconsin at La Crosse

La Crosse, WI 54601 USA

<sup>2)</sup> Independent Consultant

<sup>3)</sup>School of Mathematics and Statistics, University College Dublin

 $Belfield,\ Dublin\ 4,\ Ireland$ 

(Dated: 14 December 2022)

A novel photon-based proton model is developed. A proton's ground state is assumed to be coherent to the degree that all of its mass-energy precipitates into a single uncharged spherical structure. A quantum vortex, initiated by the strong force, but sustained in the proton's ground state by the circular Unruh effect and a spherical Rindler horizon, is proposed to confine the proton's mass-energy in its ground state. A direct connection between the circular Unruh effect, the zitterbewegung effect, spin, and general relativity is proposed. Such a structure acts as an uncharged zitterbewegung fermion, and may explain neutrino mass. A groundstate proton's central zitterbewegung fermion is assumed to be surrounded by a halo of charge shells of both signs. Virtual photon standing waves are assumed to synchronize the inner shell with the central zitterbewegung fermion. The charge shells are proposed to be associated with isospin and proton q-factor. There are only two model inputs—proton mass and quantized electronic charge—and just one adjustable parameter. The adjustable parameter, reduced only by about 0.4% from an initial estimate, provides the proton's experimentally determined magnetic moment to arbitrary precision. The resulting modeled proton charge radius agrees very well with the 2018 CODATA value. Magnetic moment and charge radius are calculated algebraically in a manner easily understood by undergraduate physics students. This proposed ground-state proton model could be considered a low-energy approximation to a full quantum chromodynamical proton model.

Keywords: quantum vortex, neutrino mass, proton charge radius, proton g-factor, circular Unruh, zitterbewegung fermion

### I. INTRODUCTION

Recent chiral effective field theory modeling has been shown to be inadequate for describing certain aspects of neutron spin at very low energies<sup>1</sup>. Chiral effective field theory<sup>2</sup> is derived from quantum chromodynamics (QCD)<sup>3</sup>. Therefore QCD itself may provide an inadequate description of both low energy neutrons and ground state protons. Hansson has argued<sup>4</sup>, that at low momentum transfers, the quarks and gluons of QCD cannot be defined and thus do not really exist within a proton.

Recent photon-based proton models, conceptually similar to those presented in this work, have been proposed<sup>5,6</sup>. However, both Niehaus<sup>6</sup> and Kovács<sup>5</sup> propose models that directly conflict with established QCD. In contrast, this work fully accepts established QCD and attempts to explain the origin of quarks, gluons, color charge, and the QCD proton's pion cloud

This work proposes that a proton, in its lowest energy (ground) state, is a completely coherent self-synchronizing structure. This may explain why a ground-state proton cannot decay. At energies above the ground state, the structure is proposed to transform into quarks and gluons according to established QCD theory.

a) Electronic mail: sverrall@uwlax.edu

This work proposes that the properties of a ground-state proton's measured projection can be derived from those of a hypothetical revolving circularly-polarized virtual photon. This virtual photon is proposed to propagate via both toroidally and poloidally revolving electromagnetic fields. The virtual photon's energy is assumed to be identical to proton mass energy. The proton's mass energy is proposed to be a quantized manifestation of the circular Unruh energy<sup>7–16</sup> of a zitterbewegung fermion. Suppose a point-like linearly-coupled Unruh-DeWitt detector circles at light speed in a massless scalar quantum field <sup>17</sup>. This work defines a zitterbewegung fermion as the superposition of such Unruh-DeWitt detectors, with a spherically uniform distribution of rotation axes.

The zitterbewegung fermion circulation is associated with the measured projection of the proton's quantized spin angular momentum. The virtual photon's poloidal revolution is associated with isospin, charge generation, and the measured projection of proton magnetic moment. The ratio of a quantum particle's projected magnetic moment to its projected spin is defined as the particle's g-factor<sup>18,19</sup>. This work offers an explanation for the proton's g-factor. Together, the virtual photon's projected toroidal and poloidal revolutions define a volume. This volume is directly related to measurements of proton charge radius.

This work models the properties of a proton's measured projection in an external approximately-uniform magnetic field. The external magnetic field is assumed to vary on scales much larger than the proton's size. It will be assumed that an electron or muon, in a proton orbital, magnetically interacts so that the proton appears to possess the properties of the modeled proton projection presented in this work. It will also be assumed that observers with no information about a proton's magnetic environment will perceive a proton to be the superposition of all possible three-dimensional orientations of the modeled proton projection. Such a superposition will be spherically symmetric.

Suppose, that in its ground state, a proton's mass-energy completely dissociates from charge and precipitates down to what appears, to inertial observers, to be a single circling point-like quasiparticle similar to a Majorana fermion. This work will refer to such a quasiparticle as a zitterbewegung fermion. This quasiparticle is proposed to contain all of a ground-state proton's spin angular momentum<sup>20</sup>. Section V explains how spacetime curvature is a necessary component of this zitterbewegung fermion model. Such a model may also explain how an uncharged neutrino can be massive without interacting with the Higgs field.

Suppose, that according to inertial observers, a ground-state proton's massless charge forms a double-shell halo structure at a considerable distance from the central zitterbewegung fermion. These two massless charge shells may be quasiparticles similar to Weyl fermions<sup>21</sup>. This double-shell charge structure is proposed to contain all of a ground-state proton's isospin<sup>22,23</sup>.

This work assumes that a ground-state proton's mass energy is quantized excess vacuum energy in the form of quantized circular Unruh energy  $^{7-16}$ . To inertial observers, a ground-state proton's mass energy is proposed to appear as a point-like particle circling at light speed. Such light-speed circular motion is called zitterbewegung motion  $^{6,24-32}$ . Zitterbewegung motion involves centripetal acceleration, which will be called zitterbewegung acceleration in this work. On subatomic scales, this work proposes that such centripetal acceleration involves the circular Unruh effect  $^{7-14}$ .

A particle circling at light speed can neither act as an observer nor be observed. However, this can conceptually act as a classical model, based on space-time algebra<sup>33</sup>, of the projection of the particle's quantum mechanical spin about a particular axis. This spin projection can be measured by inertial observers. Even after measuring spin projection, the location and momentum of the particle's center is still subject to Heisenberg's uncertainty principle<sup>34</sup>.

This work proposes, that in a ground-state proton, the space-time algebra model<sup>28,32,33</sup> of a point-like proton mass circling at light speed is equivalent to a point-like linearly-coupled Unruh-DeWitt detector, circling at light speed in a massless scalar quantum field<sup>17</sup>, with a proton's zitterbewegung acceleration. The angular momentum of this circling Unruh-DeWitt detector is assumed quantized as a spin-half fermion. The circular Unruh effect

generates thermal excess vacuum energy with a characteristic Unruh temperature  $^{7-16}$ . It is reasonable to assume that the Unruh effect is fundamentally local  $^{35}$ . It will be shown that the median energy associated with this characteristic Unruh temperature is approximately 98.9% similar to proton mass energy. It will be argued that self-synchronization with the ground-state proton's inner charge shell quantizes the Unruh energy  $^{7-16}$  as proton mass energy. This self-synchronization may be connected to the proton's unique stability.

When excited above its ground state, about 1-2% of a proton's quantized excess vacuum energy may couple with the Higgs field and transfer from the central zitterbewegung fermion to its double-shell charge structure. This may form three valence quarks, and a pion cloud, via a similar mechanism to Weyl fermions coupling with the Higgs field to form quarks<sup>36</sup>. The weak isospins of the three valence quarks sum to the proton's net isospin<sup>37</sup>. The remaining 98-99% of a proton's quantized excess vacuum energy is proposed to transform into virtual gluons and sea quarks<sup>38</sup>. The proton's spin angular momentum may partially migrate from the virtual gluons and sea quarks to the valence quarks. This partial migration may be interaction-dependent and provide a conceptual clue to the proton spin crisis<sup>39-41</sup>.

#### II. PROPOSED ZITTERBEWEGUNG QUANTUM VORTEX MOTION

This work proposes a ground-state quantum vortex (GSQV) proton model, based on aspects of the zitterbewegung interpretation of quantum mechanics<sup>6,24–32</sup>, the circular Unruh effect<sup>7–14</sup>, quantum electrodynamics, and classical electromagnetism. At energies above the ground state, this model transforms into the established QCD description of a proton derived from quantum field theory<sup>17</sup>.

Recent experimental evidence<sup>42–45</sup>, supports the concept of the zitterbewegung effect being due to stable intrinsic high frequency oscillations. In standard quantum mechanics, zitterbewegung is interpreted as the interference between positive- and negative-energy wave components. In quantum electrodynamics, the negative energy states of electron zitterbewegung are modeled as positron states<sup>46</sup>. A purely classical interpretation of the zitterbewegung effect<sup>28–32</sup> is problematic<sup>47</sup>.

This work models the zitterbewegung of an unobserved proton as the superposition of virtual photon vortices with every possible rotation axis. The observed projection of proton zitterbewegung, in an approximately uniform external magnetic field, is modeled as the toroidal revolution of a photon vortex in a plane orthogonal to the external magnetic field. It is acknowledged that the proton's spin axis will actually be in a state of Larmor precession<sup>18</sup>. However, this work models only the properties of a proton's observed projection in an external magnetic field.

Prior zitterbewegung-based particle models have generally focused on the electron<sup>24–32</sup>. Some models assume the electron to be a circling point charge co-located with the electron's mass energy<sup>24–31</sup>. Other models assume that the circling point of mass energy has an extended, but still very localized, co-moving charge structure<sup>32</sup>. These works either assume or conclude that the centripetal force required for the particle to self-circulate is electromagnetic in nature. This work proposes that a proton displays zitterbewegung motion due to a non-electromagnetic quantum vacuum interaction.

This work assumes proton mass to be intrinsic. It is set to the 2018 CODATA value. Others have long explained proton spin angular momentum and Heisenberg's uncertainty principle via the zitterbewegung interpretation of quantum mechanics<sup>28,32</sup>. This work progresses this line of reasoning and adds explanations for isospin, charge generation, charge quantization, magnetic moment, and charge radius. A similar, but far from identical, model was recently proposed<sup>6</sup>. A key difference is that the proton model proposed by Niehaus contains only positive charge<sup>6</sup>, whereas the GSQV proton model proposed in this work contains both positive and negative charge. In addition, the GSQV proton model proposed in this work explains the origin of quarks and gluons, whereas the proton model proposed by Niehaus is presented as a challenge to the established QCD theoretical framework<sup>6</sup>.

#### III. MODEL DESCRIPTION

The GSQV proton is a relatively simple structure consisting of just three parts: A central relatively-compact zitterbewegung fermion inside two massless oppositely-charged rotating shells. Proton isospin, charge generation, quantization, and circulation are explained in the context of a revolving circularly polarized virtual photon. Proton-antiproton pair production is initiated via a sufficiently energetic photon interacting with an atomic nucleus. This work assumes that the spin-1 photon initially splits into two spin-half photon vortices. Photon vortex rotation is assumed to be initiated by the strong force in the guise of a force centripetally accelerating a point-like Unruh-De-Witt detector in a massless quantum field. Each photon vortex, which will be called a quantum vortex, is assumed to be the spherically-uniform superposition of revolving circularly-polarized virtual photons. Each virtual photon of the superposition is assumed to revolve with one poloidal cycle for every two toroidal cycles.

A half poloidal cycle per toroidal cycle is assumed to be the geometrical cause of a GSQV proton's quantized half isospin. The poloidal electromagnetic field rotation rate is assumed to generate and quantize the GSQV proton's charge. How could the poloidal rotation of a revolving virtual photon's fields generate charge? It is well known that an accelerating charge generates electromagnetic radiation. This work effectively assumes that highly accelerated virtual electromagnetic fields generate charge in a quantized manner. Similar mechanisms for electron and quark charge formation have been proposed. Baixauli recently derived electron and quark charge quantization from Planck sphere rotation in a higher dimension<sup>48</sup>.

This work assumes that a GSQV proton's mass energy and angular momentum are contained in an uncharged central spherical region. The GSQV proton's charge shells are therefore assumed to carry no additional energy or angular momentum. The combined toroidal and poloidal virtual electromagnetic field flow of a GSQV proton's projected virtual photon is assumed to form a spindle torus structure. Fig. 1 shows a polar cross-sectional diagram of the projection of a GSQV proton. It will be assumed that opposing charge forms on the surfaces of two coherently rotating shells with the equatorial diameter of the inner shell precisely matching the proton's Compton wavelength,  $\lambda_c = h/mc$ , where h is Planck's constant, m is proton mass, and c is the speed of light.

The assumption that the inner shell's equatorial diameter precisely matches the proton's Compton wavelength relates a GSQV proton's magnetic moment to its size. According to classical electromagnetism, the volume inside a GSQV proton's inner shell should contain many repelling electric forces. According to quantum electrodynamics, this volume is filled with virtual photons carring electric force. This work assumes that virtual photons, precisely matching the proton's Compton wavelength, form standing waves across the inner shell's diameter. These standing waves are assumed to both maintain the charge structure of the GSQV proton and resist perturbation.

A spindle torus consists of an inner lemon surface and an outer apple surface. This work assumes a GSQV proton's inner lemon surface is negatively charged while its outer apple surface is positively charged. A GSQV antiproton is assumed to have the same charge structure, but with opposite charges. This work assumes that each of these massless charge shells coherently rotates toroidally with an equatorial speed pegged to the speed of light. In special relativity, a massless object can only move at light speed. While the charge structure is assumed to be generated by the poloidal flow of a projected virtual photon's electromagnetic fields, the charge structure itself is assumed to circulate purely toroidally with zero poloidal component. This charge motion generates the proton's magnetic moment according to classical electromagnetism. A GSQV proton's projected charge radius is assumed to be equivalent to the radius of a sphere with the same volume as the outer charge shell of the GSQV proton model.

A GSQV proton model is initially derived as a first approximation with no adjustable parameters. The GSQV proton magnetic moment is calculated to within 0.15% of the 2018 CODATA value. The GSQV proton charge radius is calculated to be about 0.64%

larger than the 2018 CODATA value. A refined GSQV proton model, with one adjustable parameter, is derived. This refined model calculates the GSQV proton magnetic moment to arbitrary precision and the GSQV proton charge radius to well within the uncertainty of the 2018 CODATA value.

There has been considerable debate over whether free protons are perfectly spherical, slightly prolate, slightly oblate, or malleable between prolate and oblate<sup>49</sup>. A subrelativistic GSQV proton should appear quite spherical to observers with no knowledge of the proton's magnetic environment. However, during very close interactions with another magnetic dipole, the GSQV proton is assumed to appear as a single slightly-oblate projection to the other magnetic dipole, as in Fig. 1. A closely interacting magnetic dipole may include another nucleon, electron, or muon. Experimental evidence for non-spherical proton-nucleon interaction was recently published by the PHENIX Collaboration<sup>50</sup>.

#### IV. QUANTIZED CIRCULAR UNRUH ENERGY

Recently, Miranda-Colón has argued that Unruh temperature represents the temperature on a quantum wave packet membrane<sup>51</sup>. This temperature is claimed to fluctuate at the zitterbewegung frequency. In contrast, this work argues that proton mass energy is equivalent to quantized circular Unruh energy due to the internal circulation of a zitterbewegung fermion.

Section V argues, that to inertial observers of a subrelativistic ground-state proton, a point-like proton mass appears to be constantly moving at light speed on a thin zitter bewegung spherical shell of radius  $r_z$ . Section VI explains why a GSQV proton's zitter bewegung radius,  $r_z$ , should be

$$r_z = \frac{\lambda_c}{4\pi} = \frac{\hbar}{2mc} \approx 0.10515 \text{ fm}, \tag{1}$$

where  $\hbar = h/2\pi$  is Planck's reduced constant. Fig. 1 shows that  $r_z$  is much smaller than the proton's charge radius. Suppose, that in a GSQV proton's central zitterbewegung fermion, a point-like linearly-coupled Unruh-DeWitt detector<sup>11,12</sup> is in light speed uniform circular motion at zitterbewegung radius,  $r_z$ . The detector's proper centripetal acceleration is given by  $a = \gamma^2 v^2/r_z$ , where v is detector speed and  $\gamma^2 = \left(1 - v^2/c^2\right)^{-1}$ . Since v = c, both  $\gamma^2$  and a are undefined.

Unruh temperature<sup>7–16</sup>, in the form of excess vacuum thermal energy, is associated with acceleration. For an Unruh-DeWitt detector<sup>11,12</sup> with proper linear acceleration, a, linear Unruh temperature is given by<sup>7–16</sup>

$$T_{\rm lin} = \frac{\hbar a}{2\pi c k_B},\tag{2}$$

where  $k_B$  is the Boltzmann constant. For an Unruh-DeWitt detector in uniform circular motion, with a very low energy gap with respect to its environment, the ratio of circular to linear Unruh temperature in the ultrarelativistic limit is given by<sup>7</sup>

$$\frac{T_{\rm circ}}{T_{\rm lin}} = \frac{\pi}{2\sqrt{3}}.\tag{3}$$

The GSQV proton's central zitterbewegung fermion is defined as the uniformly distributed superposition of zitterbewegung trajectories with all possible rotation axis orientations passing through its center. Such a superposition of Unruh-DeWitt detector trajectories will form a thin spherical shell of radius  $r_z$ . This zitterbewegung spherical shell may itself be an Unruh-DeWitt detector quantum entangled with the point-like centripetally-accelerating Unruh-DeWitt detector. In other words, each and every ensemble member may be entangled with the remainder of its ensemble.

To inertial observers, the total inward centripetal force, required to accelerate the superposition of centripetally accelerating ultrarelativistic point-like Unruh-DeWitt detectors, needs only to move at the speed of the center of zitterbewegung circulation. Therefore, for a subrelativistic proton, this required centripetal force will be proportional to zitterbewegung acceleration measured in the observer's coordinate reference frame,

$$a_z = \frac{c^2}{r_z}. (4)$$

Combining Eqns. (1) and (4) yields

$$a_z = \frac{2mc^3}{\hbar} \approx 8.547 \times 10^{32} \text{ m/s}^2$$
 (5)

for a subrelativistic proton. Combining Eqns. (2), (3), and (5) yields

$$T_{\rm circ} = \frac{\hbar a_z}{4\sqrt{3}ck_B} = \frac{mc^2}{2\sqrt{3}k_B} \approx 3.143 \times 10^{12} \text{ K}$$
 (6)

for a subrelativistic GSQV proton's central zitterbewegung fermion. This implies that a GSQV proton's mass energy,

$$E = mc^2 = 2\sqrt{3}k_B T_{\rm circ}. (7)$$

The median energy of a particle in a thermal bath at temperature, T, is given by  $^{52}$   $k_BT/0.2855$ . This appears to imply that a GSQV proton's mass energy, E, is approximately equal to  $2\sqrt{3} \times 0.2855 \approx 98.9\%$  of the median thermal excess vacuum energy due to the circular Unruh effect. A GSQV proton's quantized mass energy appears to be directly related to the thermalized Unruh energy associated with its central zitterbewegung fermion. However, as shown in Fig. 1, virtual photon standing waves, precisely matching the proton's Compton wavelength,  $\lambda_c$ , are assumed to continually pass through the GSQV proton's central zitterbewegung fermion. It will therefore be assumed that this triggers the Unruh energy of the central zitterbewegung fermion to quantize to the single frequency matching the proton's Compton wavelength. This self-synchronization may be connected to the proton's unique stability.

It has long been established that approximately 1% of a proton's mass energy is attributable to its valence quark masses. In the standard model, Weyl fermion coupling with the Higgs field generates the proton's valence quark masses. Being massless, the GSQV proton's charge shells may behave like a pair of Weyl fermions of opposing chirality. This work assumes, that when a proton is excited above its ground state, approximately 1-2% of a proton's mass energy couples with the Higgs field and transfers from its central zitterbewegung fermion to its double-shell charge structure.

At energies sufficiently elevated above the proton's ground state, this work proposes that the +2e charge of the outer GSQV proton shell evenly divides into three up quarks. Due to the Pauli exclusion principle, these three up quarks cannot be in the same quantum state. This may explain why QCD involves precisely three fundamental color charge types. In accordance with QCD, the three up quarks formed by the outer GSQV proton shell must each possess a different color charge. The right-hand column of Panel (a) in Fig. 2 represents the outer GSQV proton shell transforming into a red, a green, and a blue up-quark trio.

Since a QCD proton is color neutral, the GSQV proton's inner shell must also be color neutral. At energies sufficiently elevated above the proton's ground state, this work proposes that the -e charge of the inner GSQV proton shell divides into a down and anti-up quark pair. To maintain color neutrality, these two quarks must be a color/anti-color pair. This may explain why QCD involves three anti-color charges. The left-hand column of Panel (a) in Fig. 2 represents the inner GSQV proton shell transforming into a red down quark and an anti-red (shown as dashed red) anti-up quark. However, any color/anti-color combination is possible.

Once the GSQV proton's shells have transformed into five quarks, three can form a QCD proton, as shown below the slanted line in Panel (b) of Fig. 2. The remaining two quarks can then initiate the formation of a virtual neutral pion cloud. This may explain why a

QCD proton must possess a neutral pion cloud, and why neutral pions are color neutral. A neutral pion is one of the many two-quark particles called mesons. It is well known that all mesons are color neutral.

### V. STRONG FORCE AND GRAVITY

Consider the accelerated reference frame of the point-like Unruh-DeWitt detector described in Section IV. Since the detector is moving at light speed, it cannot act as a classical observer and its centripetal acceleration, a, is undefined. However, as the velocity of a circling object tends toward the speed of light, its centripetal acceleration tends toward infinity. For an object with acceleration tending toward infinity, its associated Rindler horizon distance  $^{13,15}$  tends toward zero.

For general centripetal acceleration, a Rindler horizon cannot form in the usually defined way<sup>53</sup>. This is because such a horizon can't act as a Killing horizon due to not being in a consistent direction relative to the rotation axis. In a circling object's accelerated reference frame, light emitted from any observable source appears to spiral into and can eventually reach the object<sup>53</sup>. However, a Rindler horizon at zero distance can conceivably act as an instantaneous Killing horizon, akin to the light surface defined in Refs. 54 and 53.

Section IV explains why the superposition of Unruh-DeWitt detector locations will form a thin zitterbewegung spherical shell of radius  $r_z$ . This work will assume that the associated superposition of instantaneous Killing horizons, at zero distance from the centripetally accelerating detector, acts as a spherical Killing horizon, of radius  $r_z$ , for the quantum vacuum inside the shell. It will be argued that observers outside this zitterbewegung spherical shell will experience spacetime curvature without perceiving the shell as a Killing horizon. The GSQV proton's central zitterbewegung fermion is therefore not a black hole.

This work models the interior of this zitterbewegung spherical shell, of radius  $r_z$ , as Minkowski spacetime. One quantum of the circular Unruh energy of the GSQV proton's central zitterbewegung fermion is assumed to be contained inside this zitterbewegung spherical shell. Unruh energy is in excess of the background vacuum energy of the immediate environment.

In Minkowski spacetime, excess energy trapped inside a volume will exert excess internal pressure, p = U/3V, where U is excess internal energy and V is volume. For the GSQV proton's zitterbewegung spherical shell,  $U = mc^2$  and  $V = \frac{4}{3}\pi r_z^3$ . Therefore excess internal pressure exerted by circular Unruh energy,

$$p = \frac{mc^2}{4\pi r_z^3}. (8)$$

The total outward force exerted by circular Unruh energy on the zitter bewegung spherical shell, F = pA, where  $A = 4\pi r_z^2$ . Therefore

$$F = \frac{mc^2}{r_z} = ma_z,\tag{9}$$

where  $a_z$  is zitterbewegung centripetal acceleration defined by Eqn. (4). Clearly F is the total inward force required to generate the required centripetal acceleration, needed to contain the GSQV proton's mass energy inside its central zitterbewegung fermion, and to balance the zitterbewegung spherical shell's excess internal vacuum pressure due to circular Unruh energy. In this GSQV proton model, this force plays the role of the strong force. Applying inertial and gravitational mass equivalence, it will be assumed that spacetime curvature, described by general relativity, causes the total inward surface pressure, p, required to stabilize the zitterbewegung spherical shell.

The point-like Unruh-DeWitt detector described in Section IV travels at the speed of light. It therefore cannot act as an observer because it experiences extreme time dilation to the degree that time does not elapse at all. If it attempted to act as an observer, it would observe nothing. To an object traveling at light speed, the observable Universe would be

nothing other than the point of its location. However, distances of zero length may be physically impossible. Suppose that the point-like Unruh-DeWitt detector is actually a sphere of radius  $\sqrt{2}\ l_p$ , where  $l_p\approx 1.616\times 10^{-35}$  m is the Planck length<sup>55</sup>. The circling Unruh-DeWitt detector's cross-sectional area will then be  $2\pi l_p^2$ .

This Unruh-Dewitt detector is always located somewhere on the surface of the zitterbewegung spherical shell. The inward gravitational force due to pressure,  $p_g = mc^2/4\pi r_z^3$ , exerted by curved spacetime on this Unruh-DeWitt detector, will be assumed to be cross-sectional area,  $2\pi l_p^2$ , multiplied by the pressure exerted by spacetime curvature:

$$F_g = 2\pi l_p^2 p_g = \frac{mc^2 l_p^2}{2r_z^3} = \frac{Gmm_p l_p}{2r_z^3} = \frac{Gm^2}{r_z^2},$$
(10)

since  $c^2 = Gm_p/l_p$  and  $m_pl_p/r_z = \hbar/cr_z = 2m$ , where  $m_p$  is the Planck mass. The Unruh-DeWitt detector therefore experiences a force, due to curved spacetime, as if it were a point-like proton mass, m, in the Newtonian gravitational field of another apparent point-like proton mass at the center of the zitterbewegung spherical shell. The same effect would result if the apparent point-like proton mass, at the center of the zitterbewegung spherical shell, was actually uniformly distributed on a thin spherical shell of radius  $\leq r_z$ . This structure would have zero interior gravitational field and zero spacetime curvature, but the same exterior spacetime curvature as that of a point-like proton mass.

It is therefore appropriate to model the zitterbewegung spherical shell's interior as Minkowski spacetime, as was assumed when deriving Eqn. (8). The geometries of the two apparent proton masses: one point-like; the other uniformly distributed on a spherical shell of radius,  $r_z$ , are the same as the two quantum entangled Unruh-DeWitt detectors described in Section IV.

One way to visualize why the gravitational force, described by Eqn. (10), is so much weaker than the centripetal force, described by Eqn. (9), is that curved spacetime must always be capable of attracting a spherical Unruh-DeWitt detector, of radius  $\sqrt{2} \ l_p$ , at any location on any possible trajectory on the zitterbewegung sphere. This is assumed to be because spacetime curvature, caused by a zitterbewegung fermion's confined mass energy, cannot determine a priori the location of an Unruh-DeWitt detector circling at light speed. It is therefore incapable of applying pressure only in the momentary direction of the circling point-like Unruh-DeWitt detector. Spacetime curvature, due to a zitterbewegung fermion, must therefore always be spherically symmetric.

Another way to interpret Eqn. (10) is that the light-speed circling Unruh-DeWitt detector's effective mass is evenly diluted over the zitterbewegung sphere by the factor  $2\pi l_p^2/4\pi r_z^2 = l_p^2/2r_z^2$ . In the coordinate reference frame of a subrelativistic GSQV proton, the centripetal force required to keep this diluted mass circling at light speed,

$$F_c = \frac{ml_p^2}{2r_z^2} \frac{c^2}{r_z} = \frac{Gm^2}{r_z^2} = F_g, \tag{11}$$

which shows that the exceptionally weak inward gravitational force on the zitterbewegung sphere maintains the centripetal force required for zitterbewegung motion.

This work therefore claims that the apparent zitterbewegung of a ground state proton is due to the combined effects of general relativity and the circular Unruh effect derived from quantum field theory. The strong force, as described by QCD, does not become apparent until a GSQV proton gains enough energy to form valence quarks. It is well known that quarks obtain mass via Higgs field interaction. However, the Higgs mechanism does not explain neutrino mass formation. The zitterbewegung fermion model, proposed in this work, occurs independently of charge and thus may also serve as a neutrino mass model.

### VI. MASS DYNAMICS

Section V argued, that to inertial observers of a subrelativistic ground-state proton, a point-like proton mass appears to be constantly moving at light speed on a thin zitterbe-

wegung spherical shell of radius  $r_z$ . It will be shown that

$$r_z = \frac{\hbar}{2mc} = \frac{\lambda_c}{2},\tag{12}$$

since  $\lambda_c = \hbar/mc$  and  $\lambda_c = \lambda_c/2\pi$  is a proton's reduced Compton wavelength, is consistent with both Heisenberg's uncertainty principle and spin-half angular momentum.

In the coordinate reference frame, of an observer co-moving with the center of zitterbewegung circulation, the magnitude of the momentum of a GSQV proton's point-like circling mass appears to be

$$p_z = mc = \frac{\hbar}{2r_z} = \frac{\hbar}{\lambda_c}. (13)$$

Combining Eqns. (12) and (13) yields spin angular momentum.

$$L = p_z r_z = \frac{\hbar}{\lambda_c} \frac{\lambda_c}{2} = \frac{\hbar}{2}.$$
 (14)

This is the intrinsic angular momentum for all spin-half particles, including low energy protons.

It is well known that the quantum mechanical spin of a free spin-half particle appears to be the superposition of all possible spin axis orientations. Therefore, according to inertial observers, the position of the point-like mass of a GSQV proton can be modeled as randomly varying on the surface of a sphere of radius  $r_z = \lambda_c/2$ .

A light-speed particle constrained to move on a spherical surface will be at an indeterminate position on that surface. The probability distribution of its location will be uniform on that surface. Therefore the position of the apparent point-like mass of a GSQV proton on a sphere of radius  $r_z = \lambda_c/2$  is indeterminate. A GSQV proton's zitterbewegung motion is therefore not deterministic to inertial observers.

In each of the three spatial dimensions, the uncertainty of a GSQV proton's position will be  $\pm r_z$  and its uncertainty in momentum, a vector quantity, will be  $\Delta p = \pm p_z$ . This satisfies Heisenberg's position-momentum uncertainty principle, since

$$(\pm r_z)(\pm p_z) = \pm r_z p_z = \pm \frac{\lambda_c}{2} \frac{\hbar}{\lambda_c} = \pm \frac{\hbar}{2}$$
 (15)

in each of the three spatial dimensions.

#### VII. CHARGE GENERATION AND DISTRIBUTION

This work assumes that charge is generated by the poloidal rotation of the electromagnetic fields of a revolving virtual photon that is circularly polarized. Net charge is assumed to be quantized due to precisely half a poloidal turn occurring each cycle. This is independent of Compton wavelength and therefore rest mass. The poloidal cycling itself may be geometrically equivalent to proton isospin.

This work assumes that a GSQV proton's charge structure exists on the surfaces of a spindle torus. The outer apple surface is assumed to be purely positively charged while the inner lemon surface is assumed to be purely negatively charged. Fig. 1 shows a polar cross-sectional diagram of the proposed GSQV proton. A GSQV antiproton is assumed to have the same structure, but with oppositely charged surfaces.

To a first approximation, it will be assumed that the total charge on each shell is proportional to the shell's volume. This assumption has been found to yield numerically accurate results. Classically, if a volume is the source of free charges of like signs, these free charges will tend to accumulate on the volume's surface. This model will be refined so that charge quantization occurs on each charge shell. This work assumes each charge shell toroidally rotates as a coherent structure, with the equator moving at the speed of light.

Planck charge,  $q_P = \sqrt{4\pi\epsilon_0\hbar c} = e/\sqrt{\alpha}$ , where  $\epsilon_0$  is the electric permittivity of free space, e is the magnitude of quantized electronic charge, and  $\alpha$  is the fine structure constant, is the only base Planck unit that does not depend on the gravitational constant. It is therefore reasonable to propose that a particle's charge could exist spatially dissociated from its mass. It is proposed that such a mass-charge dissociation can only occur in very low energy interactions and that free massless charged particles cannot exist. At higher energies, the GSQV proton is assumed to transform into a quark-gluon structure and be well described by QCD.

This work assumes the lemon surface's equatorial diameter is the proton's Compton wavelength,  $\lambda_c = h/mc$ , where h is Planck's constant. This is shown in Fig. 1. Quantum electrodynamics (QED) assumes that electric force is carried by virtual photons. This work assumes that many virtual photon standing waves of Compton wavelength propagate across the lemon's equator.

#### VIII. MAGNETIC MOMENT AND CHARGE RADIUS

The nuclear magneton is defined as

$$\mu_N = \frac{e\hbar}{2m} = \frac{ce\lambda_c}{2} = cer_z. \tag{16}$$

Magnetic moment,  $\mu$ , is a measure of the overall magnetic field strength of a magnetic dipole. It is well known that a uniformly charged spherical shell of charge Q and radius r, rotating with angular speed  $\omega$ , has magnetic moment,  $\mu = Q\omega r^2/3$ . This work assumes equatorial speed to be pegged at the speed of light:  $\omega = c/r$ . Therefore a uniformly charged spherical shell has magnetic moment

$$\mu = \frac{Qcr}{3} = \frac{Qr}{3er_z}cer_z = \frac{Qr}{3er_z}\mu_N = \frac{QV}{er_zA}\mu_N,\tag{17}$$

where  $V = \frac{4}{3}\pi r^3$ ,  $A = 4\pi r^2$ , and V/A = r/3 for a sphere.

Suppose that a perturbed spherical shell has a charge distribution equivalent to a radially-projected uniformly-charged sphere. Such a shell, with its equator rotating at light speed, will be assumed to have magnetic moment,

$$\mu = \frac{QV}{4\pi R_E^2 e r_z} \mu_N,\tag{18}$$

where  $R_E$  is the shell's equatorial radius.

In the GSQV proton model, to a first approximation, the surface charge on each shell is assumed to depend on its volume. Each shell is assumed to have a charge distribution equivalent to a radially-projected uniformly-charged sphere.

The GSQV proton has two charge shells. To a first approximation,

$$\mu_p = \frac{Q_o V_o}{4\pi R_{Eo}^2 e r_z} \mu_N + \frac{Q_i V_i}{4\pi R_{Es}^2 e r_z} \mu_N = \left(\frac{Q_o V_o}{R_{Eo}^2} + \frac{Q_i V_i}{R_{Ei}^2}\right) \frac{\mu_N}{4\pi e r_z},\tag{19}$$

where p denotes proton, o denotes outer, and i denotes inner.

Suppose a circling point-like mass travels two cycles in a proton's Compton wavelength. The radius of this loop will be  $r_z = \lambda_c/4\pi = 0.10515$  fm. As shown in Fig. 1, the radius of each circle in the polar cross-sectional diagram of the GSQV proton,

$$R = \frac{\lambda_c}{2} + r_z = 0.76585 \text{ fm.}$$
 (20)

Therefore, the equatorial radius of the outer apple surface will be given by  $R_{Eo} = R + r_z$  and the equatorial radius of the inner lemon surface will be given by  $R_{Ei} = R - r_z$ .

The Appendix explains:  $\phi_m = \phi_l = \cos^{-1}(r_z/R) = 1.4331$  for the inner lemon surface of a spindle torus;  $\phi_m = \phi_a = \pi - \cos^{-1}(r_z/R) = 1.7085$  for the outer apple surface of a

spindle torus. The half-angles,  $\phi_l$  and  $\phi_a$ , are shown in Fig. 1. These half-angles can be interpreted as the maximum geodetic latitude on each surface. The Appendix outlines a proof that both the lemon and apple volumes may be calculated from Eqn. (A.4). Applying Eqn. (A.4): the GSQV proton's inner lemon volume,  $V_i = 1.3260 \text{ fm}^3$ ; the GSQV proton's outer apple volume,  $V_o = 2.5434 \text{ fm}^3$ . The radius of a sphere with volume  $V_o$  is given by

$$r_s = \sqrt[3]{\frac{3}{4\pi}V_o} = 0.8468 \text{ fm.}$$
 (21)

This is about 0.64% larger than the 2018 CODATA value for proton RMS charge radius: 0.8414 fm.

To a first approximation, charge is assumed proportional to shell volume:

$$\frac{Q_o}{Q_i} = -\frac{V_o}{V_i}. (22)$$

Proton net charge +e implies

$$Q_o + Q_i = e. (23)$$

Combining Eqns. (22) and (23) yields

$$Q_o = \frac{eV_o}{V_o - V_i} = 2.0892e$$
 and  $Q_i = e - Q_o = -1.0892e$ . (24)

Therefore the GSQV proton's projected magnetic moment can be calculated:

$$\mu_p = \left(\frac{Q_o V_o}{(R + r_z)^2} + \frac{Q_i V_i}{(R - r_z)^2}\right) \frac{\mu_N}{4\pi e r_z} = 2.7968 \mu_N.$$
 (25)

This is within 0.15% of the experimental 2018 CODATA value of  $\mu_p = 2.7928 \mu_N$ .

### IX. REFINED GROUND STATE QUANTUM VORTEX PROTON MODEL

Applying the right-hand rule for magnetic force from classical electromagnetism, it will be assumed that the self-interaction of the charge shell electric currents with the GSQV proton's dipolar magnetic field provides an inward force on the equatorial regions of both charge shells. It will also be assumed that virtual photons maintain a standing wave of wavelength  $\lambda_c$  across the inner shell's equatorial diameter, and that this completely prevents the inner shell's equator from compressing. It will therefore be assumed that the proton's magnetic field compresses only the outer shell's equatorial diameter. This assumption justifies making R, shown in Fig. 1, an adjustable parameter. Note that this will be the lone adjustable parameter, and that the adjustment will be only about 0.4%.

In polar regions, applying the right-hand rule for magnetic force from classical electromagnetism, it will be assumed that the proton's dipolar magnetic field provides an outward force on the positively charged outer shell and an inward force on the negatively charged inner shell. It will be assumed that these forces cause the charge shells to separate. This prevents opposing charges from being extremely close together, which avoids the possibility of extremely large attractive electrostatic forces.

It will be assumed that a positive-charge polar exclusion zone extends out to the outer shell's maximum axial range. This is indicated by the tip of the upper R arrow in Fig. 1. This implies that both positive and negative charge generation, caused by the poloidal flow of the revolving virtual photon's electromagnetic fields, involve omnidirectional flow in the axial direction. In particular, the inner shell's charge is assumed to be generated by poloidal electromagnetic field rotation in one axial direction (e.g. up), while the outer shell's charge is assumed to be generated by poloidal electromagnetic field rotation in the opposing axial direction (e.g. down).

It will be assumed that the inner shell's charge is quantized to -e and the outer shell's charge is quantized to +2e. It will be assumed that the apparent uncharged circling mass maintains its circular path of radius  $r_z = \lambda_c/4\pi$ . This makes sense, since changing the GSQV proton's zitterbewegung radius would imply also changing its inertial mass and spacetime curvature.

The value of R is optimized so that  $\mu_p = 2.7928\mu_N$ , which agrees with the 2018 CODATA value to five significant digits. Note that R may be optimized to provide  $\mu_p$  to arbitrary precision. However, the analysis shown below is limited to five significant digits. This is because the most accurate proton charge radius estimates to date are limited to four or fewer significant digits.

Define radius of polar charge exclusion zone,

$$r_a = R - \lambda_c/2,\tag{26}$$

which differs from  $r_z$  as R is adjusted. The outer charge shell is now modeled as a semicircle revolved about flat polar caps. The surface area will be slightly less than the corresponding apple surface area, while the volume will be slightly larger than the corresponding apple volume. The Appendix outlines a proof that the outer shell surface area,  $A_o$ , is now given by Eqn. (A.6) and the outer shell volume,  $V_o$ , is now given by Eqn. (A.7). Proportion of outer shell surface area with no charge,

$$Q_{\rm ex} = \frac{2\pi r_a^2}{A_o}. (27)$$

Define

$$\mu_p = \left(\frac{2V_o}{(1 - Q_{\text{ex}})(R + r_a)^2} - \frac{V_i}{(R - r_a)^2}\right) \frac{\mu_N}{4\pi r_z}.$$
 (28)

The optimized value of R=0.76273 fm provides  $\mu_p=2.7928\mu_N$ , which agrees with the 2018 CODATA value to five significant digits. This optimized R value is only about 0.4% below that given by Eqn. (20). The optimized outer shell surface area is given by Eqn. (A.6):  $A_o=8.9120~{\rm fm}^2$ . The equivalent apple surface area is 8.9121 fm², as calculated from Eqn. (A.3) with  $\phi_m=\cos^{-1}(r_a/R)$ . This differs negligibly from  $A_o$ . The optimized value of  $Q_{\rm ex}=7.339\times 10^{-3}=0.7339\%$ . The optimized outer shell volume is given by Eqn. (A.7):  $V_o=2.49434~{\rm fm}^3$ . The equivalent apple volume is 2.49427 fm³, as calculated from Eqn. (A.4) with  $\phi_m=\pi-\cos^{-1}(r_a/R)$ . This differs neglibly from  $V_o$ .

The radius of a sphere with volume  $V_o$  is given by

$$r_s = \sqrt[3]{\frac{3}{4\pi}V_o} = 0.8413 \text{ fm},$$
 (29)

which compares very well with the 2018 CODATA proton RMS charge radius of 0.8414(19) fm. Note that this GSQV proton model could be falsified by future experimental estimates of proton charge radius.

Adjusting  $Q_{\rm ex}$  by  $\pm 20\%$ , and reoptimizing R so that Eqn. (28) provides  $\mu_p = 2.7928 \mu_N$ , generates the 2018 CODATA standard uncertainty in proton RMS charge radius. Inserting these reoptimized R values into Eqn. (26) yields a  $\pm 10\%$  uncertainty in polar charge exclusion radius,  $r_a = 0.10 \pm 0.01$  fm.

#### X. COMPARISON WITH P+AU COLLISION ANALYSIS

The PHENIX Collaboration analyzed the collision of a proton with a gold nucleus<sup>50</sup>. They report surprisingly long lived and quite elliptical impact patterns. They found hydrodynamical models, which have long been used to model plasma behavior, provide the best description of their measurements. The GSQV proton model presented in this work is in a sense a stable current-carrying plasma double layer system<sup>56</sup>. However, a major

conceptual difference is that the charge shells in the GSQV proton model are not comprised of independent charged massive particles. It is therefore inappropriate to model them as a hydrodynamical plasma system.

Both charge shells in the GSQV proton are almost spherical and almost uniformly charged. To a first approximation, this system could perhaps be treated as a spherical capacitor. A charged spherical capacitor will store energy. However, the shells of the GSQV proton are massless. It requires no force to reposition classical massless particles, which implies they can't store potential energy. Both charge shells are necessarily associated with a central zitterbewegung fermion containing all of the GSQV proton's mass energy. The charge shells therefore cannot behave as independent charged massive particles. This work therefore claims that no additional energy is stored in the GSQV proton's electric field.

The elongated elliptical-like impact patterns of highly energetic p+Au collisions, shown in Fig. 1b of Ref. 50, could perhaps be explained by the intrinsically oblate GSQV proton undergoing a magnetic equatorial slide during the initial phase of the collision. When the magnetic equators of two attracting magnetic dipoles closely approach, there is far less resistance to equatorial slide than movement along the polar axes. This is easily demonstrated using any two oval or spherical magnetic dipoles. Therefore a GSQV proton model, with substantial equatorial slide, is consistent with the elongated aspect of the PHENIX Collaboration's published analysis of the collision of a proton with a gold nucleus<sup>50</sup>.

#### XI. DISCUSSION

A ground-state proton model, which accurately calculates both projected magnetic moment and charge radius, has been developed. This GSQV proton model has only two model inputs—proton mass and quantized electronic charge—and one adjustable parameter, R, shown in Fig. 1. This model offers geometric explanations for ground-state mass-energy confinement, projected spin angular momentum, proton isospin, and charge quantization. It provides a mechanism for sourcing proton quark mass energies from the local quantum vacuum. This model explains why QCD invloves three color charges and why a QCD proton possesses a pion cloud. The zitterbewegung fermion model, developed in this work, may also explain how neutrinos can possess mass without involving charge.

The GSQV proton model offers hints as to why nature prefers the proton mass over other particle masses. Assuming the two charge shells remain quantized as +2e and -e, increasing/decreasing a GSQV proton's mass energy would reduce/increase its zitterbewegung radius,  $r_z$ . This would decrease/increase shell separation, which could conceivably lead to electromagnetic instability. However, an explanation as to why the GSQV proton's charge shells are uniquely stable is not offered in this work.

The GSQV proton model's assumptions come from a variety of existing theories, both quantum and classical. The GSQV proton model relies on the existence of the vacuum of quantum field theory, which yields the circular Unruh effect upon particle rotation. A direct connection between the circular Unruh effect, the zitterbewegung effect, and general relativity was proposed in Sections IV-VI. Proton magnetic moment and charge radius were calculated classically in Sections VIII and IX.

In this GSQV proton model, the strong force is in the guise of a centripetal force. It is assumed to initiate quantum vortex rotation during pair production, and transform into the QCD-defined strong force, when the GSQV proton gains enough energy to form valence quarks. The GSQV proton model does not require the additional hidden dimensions of string theory.

The proton models of lattice QCD are extremely complex structures that require supercomputers to analyze. In stark contrast, the GSQV proton model, directly applicable only in very low energy situations, has only three parts. It could be considered a low-energy approximation to a full QCD proton model. The GSQV proton's magnetic moment and charge radius are calculated algebraically in a manner easily understood by undergraduate physics students. This proposed GSQV proton model could be falsified by future experimental

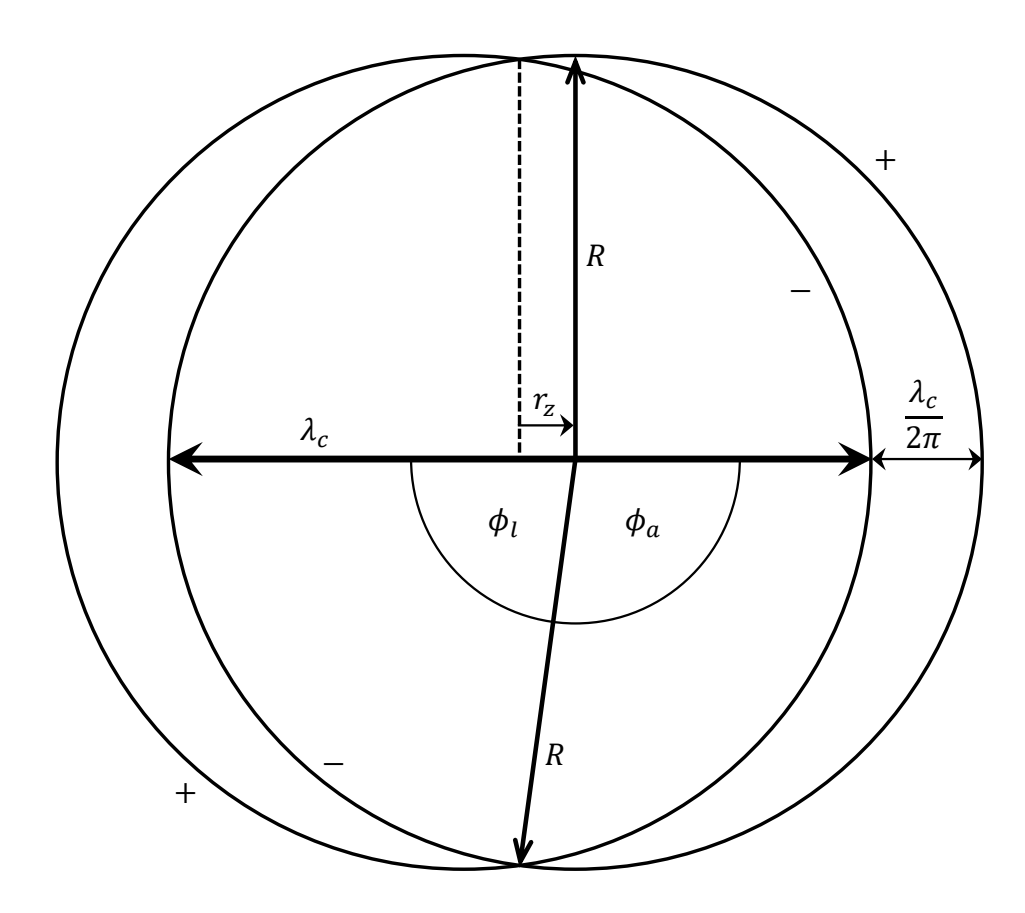


FIG. 1. Polar cross-section of the spindle torus charge structure of the GSQV proton, where  $\lambda_c$  is Compton wavelength,  $r_z = \lambda_c/4\pi$  is zitterbewegung radius,  $R = \lambda_c/2 + r_z$ ,  $\phi_l = \cos^{-1}(r_z/R)$ , and  $\phi_a = \pi - \phi_l$ 

estimates of proton charge radius.

The GSQV proton model could be incorporated as a teaching tool in much the same way that the Bohr model is still used to teach introductory quantum physics. Doing so could make quantum physics intellectually accessible to a much wider segment of the lay population. This would ultimately benefit the physics community.

# **ACKNOWLEDGMENTS**

The authors declare no conflicts of interest. Steven C. Verrall is the primary author. Micah Atkins and Andrew Kaminsky are assistant authors. Peter Lynch coauthored the Appendix. Steven C. Verrall is partly supported by UWL Faculty Research Grant 23-01-SV. Steven C. Verrall, Kelly S. Verrall, Micah Atkins, and Andrew Kaminsky developed the original concepts. Micah Atkins, Emily Friederick, and Andy Otto assisted with mathematical development and calculations.

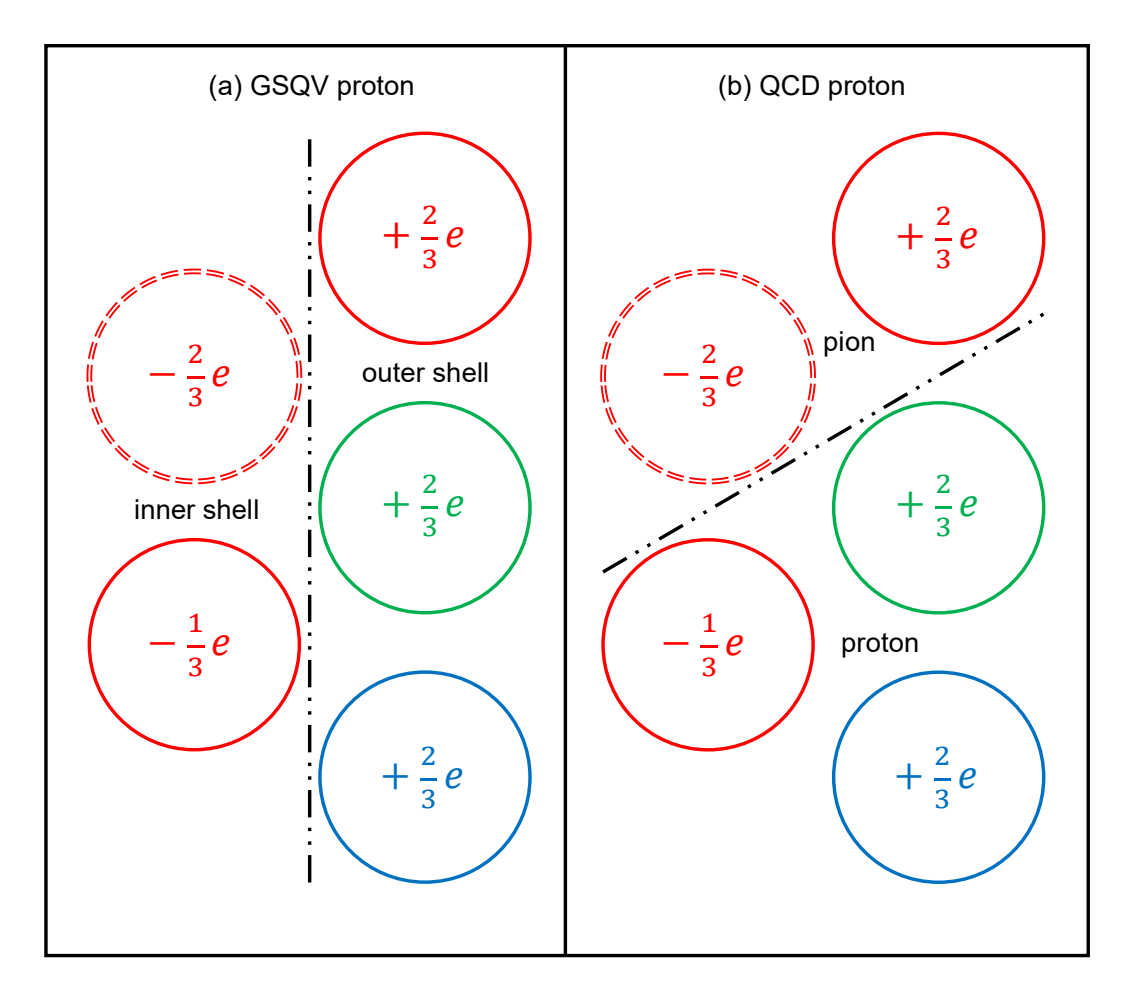


FIG. 2. Transition from GSQV to QCD proton model. Each circle represents a quark. a, The three quarks in the right-hand column are formed from the outer +2e charge shell of the GSQV proton. The two quarks in the left-hand column are formed from the inner -e charge shell of the GSQV proton. The inner charge shell is shown transitioning to a quark pair with red and anti-red (shown as dashed red) color charge. The inner shell may alternatively transition to green and anti-green or blue and anti-blue color charge pairs. b, The same five quarks in Panel (a) reorganize. The quark pair above the slanted line form a neutral pion. A neutral pion is shown formed from a quark pair with red and anti-red (shown as dashed red) color charge. The neutral pion may alternatively be formed by a green and anti-green or blue and anti-blue quark pair. The three quarks below the slanted line form a QCD proton. The inner shell, outer shell, GSQV proton, pion, and QCD proton each possess neutral color charge.

# Appendix: Volume and surface area derivations

A spindle torus consists of an inner lemon surface and an apple outer surface. The polar cross-section of a spindle torus is shown in Fig. 1. The lemon is generated by rotating an arc of half-angle  $\phi_m$  less than  $\pi/2$  about its chord, with  $\phi_m = \phi_l = \cos^{-1}(r_z/R)$ . The half-angle,  $\phi_l$ , is shown in Fig. 1. Note that  $\phi$  denotes geodetic latitude, as used in geophysics. It does not denote the azimuthal angle of conventional physics spherical coordinates. The surface area is given by

$$A = 2\pi R^2 \int_{-\phi_m}^{\phi_m} (\cos \phi - \cos \phi_m) d\phi. \tag{A.1}$$

The volume is given by

$$V = \pi R^3 \int_{-\phi_m}^{\phi_m} (\cos \phi - \cos \phi_m)^2 \cos \phi d\phi. \tag{A.2}$$

These integrals can be evaluated analytically, giving

$$A = 4\pi R^2 (\sin \phi_m - \phi_m \cos \phi_m) \tag{A.3}$$

$$V = \frac{4}{3}\pi R^3 \left[ \sin^3 \phi_m - \frac{3}{4}\cos \phi_m (2\phi_m - \sin 2\phi_m) \right]$$
 (A.4)

The apple is generated by rotating an arc of half-angle  $\phi_m$  greater than  $\pi/2$  about its chord, with  $\phi_m = \phi_a = \pi - \cos^{-1}(r_z/R) = \pi - \phi_l$ . The half-angle,  $\phi_a$ , is shown in Fig. 1. Note that Eqns. (A.3) and (A.4) are valid for both the lemon and apple.

With the refined GSQV proton model, R becomes an adjustable parameter. The quantity  $r_z$  is replaced by the radius of the polar charge-exclusion zone,

$$r_a = R - \lambda_c/2. \tag{A.5}$$

The outer charge shell is modeled as a semicircle revolved about flat polar caps. Pappus's centroid theorems are applied. The area of a surface of revolution, generated by rotating a plane curve about an external axis in the same plane, is equal to the product of the arc length of the curve and the distance travelled by the centroid of the curve. In this case, the curve is a semicircular arc with centroid located  $2R/\pi$  more distant than  $r_a$ . The arc length of the semicircle is  $\pi R$ , and the distance travelled by the centroid is  $2\pi(r_a + 2R/\pi)$ . The area of each endcap is  $\pi r_a^2$ . Therefore, including both endcaps, the outer shell surface area is given by

$$A_o = 2\pi^2 R \left( r_a + \frac{2R}{\pi} \right) + 2\pi r_a^2. \tag{A.6}$$

The volume of a solid of revolution, generated by rotating a plane figure about an external axis in the same plane, is equal to the product of the area of the figure and the distance travelled by its centroid. In this case, the plane figure is a semicircular area with centroid located  $4R/3\pi$  more distant than  $r_a$ . The area of the semicircle is  $\pi R^2/2$ , and the distance travelled by the centroid is  $2\pi(r_a+4R/3\pi)$ . The cylindrical volume between the two endcaps is  $2\pi r_a^2 R$ . Therefore, the outer shell volume is given by

$$V_o = \pi^2 R^2 \left( r_a + \frac{4R}{3\pi} \right) + 2\pi r_a^2 R. \tag{A.7}$$

<sup>&</sup>lt;sup>1</sup>V. Sulkosky et al., "Measurement of the generalized spin polarizabilities of the neutron in the low-q2 region," Nature Physics 17, 687–692 (2021).

<sup>&</sup>lt;sup>2</sup>V. Bernard, N. Kaiser, and Ulf-G. Meißner, "Chiral dynamics in nucleons and nuclei," Int. J. Mod. Phys. E 4, 193–344 (1995).

<sup>&</sup>lt;sup>3</sup>J. Greensite, An Introduction to the Confinement Problem (Springer, Germany, 2011).

<sup>&</sup>lt;sup>4</sup>J. Hansson, "A simple explanation of the non-appearance of physical gluons and quarks," Can. J. Phys. 80, 1093–1097 (2002).

 <sup>&</sup>lt;sup>5</sup>A. Kovács, "Maxwell-Dirac Theory and Occam's Razor: Unified Field, Elementary Particles, and Nuclear Interactions," (2019) Chapter "The Electromagnetic Wave Equation Based Nuclear Model", pp. 101–130.
 <sup>6</sup>A. Niehaus, "Trying an Alternative Ansatz to Quantum Physics," Found. Phys. **52** (2022).

<sup>&</sup>lt;sup>7</sup>S. Biermann, S. Erne, C. Gooding, J. Louko, J. Schmiedmayer, W. G. Unruh, and S. Weinfurtner, "Unruh and analogue Unruh temperatures for circular motion in 3 + 1 and 2 + 1 dimensions," Phys. Rev. D **102** (2020).

<sup>&</sup>lt;sup>8</sup>K. Lochan, H. Ulbricht, A. Vinante, and S. K. Goyal, "Detecting Acceleration-Enhanced Vacuum Fluctuations with Atoms Inside a Cavity," Phys. Rev. Lett. 125 (2020).

<sup>&</sup>lt;sup>9</sup>M. H. Lynch, E. Cohen, Y. Hadad, and I. Kaminer, "Experimental observation of acceleration-induced thermality," Phys. Rev. D 104 (2021).

<sup>&</sup>lt;sup>10</sup>G. Matsas, "The Fulling-Davies-Unruh Effect is Mandatory: The Proton's Testimony," Int. J. Mod. Phys. D 11, 1573–1577 (2002).

<sup>&</sup>lt;sup>11</sup>B. S. Dewitt, "Quantum gravity: the new synthesis." in General Relativity: An Einstein centenary survey, edited by S. W. Hawking and W. Israel (1979) pp. 680–745.

<sup>&</sup>lt;sup>12</sup>W. G. Unruh, "Notes on black-hole evaporation," Phys. Rev. D **14**, 870–892 (1976).

<sup>&</sup>lt;sup>13</sup>P. C. W. Davies, "Scalar production in Schwarzschild and Rindler metrics," J. Phys. A 8, 609–616 (1975).

- <sup>14</sup>S. A. Fulling, "Nonuniqueness of Canonical Field Quantization in Riemannian Space-Time," Phys. Rev. D 7, 2850–2862 (1973).
- <sup>15</sup>S. Takagi, "Vacuum Noise and Stress Induced by Uniform Acceleration: Hawking-Unruh Effect in Rindler Manifold of Arbitrary Dimensions," Progress of Theoretical Physics Supplement 88, 1–142 (1986).
- <sup>16</sup>W. G. Unruh, "Physics meets Philosophy at the Planck Scale," (Cambridge University Press, 2001) Section "Black holes, dumb holes, and entropy", pp. 152–173.
- <sup>17</sup>M. Peskin and D. Schroeder, An Introduction to Quantum Field Theory (Westview Press, 1995).
- <sup>18</sup>M. H. Levitt, Spin Dynamics: Basics of Nuclear Magnetic Resonance (Wiley, 2001).
- <sup>19</sup>Y. Peleg, R. Pnini, E. Zaarur, and E. Hecht, Schaum's outline of theory and problems of quantum mechanics, 2nd ed. (McGraw-Hill, New York, 2010).
- <sup>20</sup>P. A. M. Dirac, "The quantum theory of the electron," Proc. R. Soc. Lond. A 17, 610–624 (1928).
- <sup>21</sup>H. Weyl, "Elektron und Gravitation. I," Zeitschrift für Physik **56**, 330–352 (1929).
- <sup>22</sup>W. Heisenberg, "Über den Bau der Atomkerne," Zeitschrift für Physik 77, 1–11 (1932).
- <sup>23</sup>E. Wigner, "On the Consequences of the Symmetry of the Nuclear Hamiltonian on the Spectroscopy of Nuclei," Phys. Rev. 51, 106–119 (1937).
- <sup>24</sup>G. Breit, "An Interpretation of Dirac's Theory of the Electron," Proceedings of the National Academy of Sciences 14, 553–559 (1928).
- <sup>25</sup>W. Greiner, Relativistic Quantum Mechanics, 3rd ed. (Springer, Germany, 1995).
- <sup>26</sup>E. Schrödinger, "Über die kräftefreie Bewegung in der relativistischen Quantenmechanik," (Berlin, 1930) pp. 418–428.
- <sup>27</sup>E. Schrödinger, "Zur quantendynamik des elektrons," (Berlin, 1931) pp. 63–72.
- <sup>28</sup>D. Hestenes, "The zitterbewegung interpretation of quantum mechanics," Found. Phys. **20**, 1213–1232 (1990).
- <sup>29</sup>D. Hestenes, "Zitterbewegung in quantum mechanics," Found. Phys. **40**, 1–54 (2010).
- <sup>30</sup>A. O. Barut and N. Zanghi, "Classical Model of the Dirac Electron," Phys. Rev. Lett. 52, 2009–2012 (1984).
- <sup>31</sup>A. Niehaus, "A Probabilistic Model of Spin and Spin Measurements," Found. Phys. **46**, 3–13 (2016).
- <sup>32</sup>A. Kovács, G. Vassallo, A. O. Di Tommaso, F. Celani, and D. Wang, Maxwell-Dirac Theory and Occam's Razor: Unified Field, Elementary Particles, and Nuclear Interactions (2019).
- $^{33}\mathrm{D.}$  Hestenes,  $Space\text{-}Time\ Algebra,\ 2nd\ ed.\ (Birkhäuser,\ 2015).$
- <sup>34</sup>D. Sen, "The uncertainty relations in quantum mechanics," Current Science **107**, 203–218 (2014).
- <sup>35</sup>C. Anastopoulos and N. Savvidou, "Coherences of accelerated detectors and the local character of the Unruh effect," J. Math. Phys. **53** (2012).
- <sup>36</sup>M. Shifman, ITEP Lectures on Particle Physics and Field Theory, Vol. 1 (World Scientific, 1999) p. 292.
- <sup>37</sup>J. C. Baez and J. Huerta, "The algebra of grand unified theories," Bull. Am. Math. Soc. **47**, 483–552 (2009)
- <sup>38</sup>B. Pvoh, C. Scholz, K. Rith, and F. Zetsche, Particles and Nuclei (Springer, 2008) p. 98.
- <sup>39</sup>E. Leader and M. Anselmino, "A crisis in the parton model: Where, oh where is the proton's spin?" Z. Phys. C 41, 239–246 (1988).
- <sup>40</sup>J. Ashman et al., "A measurement of the spin asymmetry and determination of the structure function g1 in deep inelastic muon-proton scattering," Phys. Lett. B 206, 364–370 (1988).
- <sup>41</sup>J. Hansson, "The "Proton Spin Crisis" a Quantum Query," Prog. Phys. **3**, 51–52 (2010).
- <sup>42</sup>P. Catillon, N. Cue, M. J. Gaillard, et al., "A Search for the de Broglie Particle Internal Clock by Means of Electron Channeling," Found. Phys. 38, 659–664 (2008).
- <sup>43</sup>C. Wunderlich, "Trapped ion set to quiver," Nature **463**, 37–39 (2010).
- <sup>44</sup>R. Gerritsma *et al.*, "Quantum simulation of the dirac equation," Nature **463**, 68–71 (2010).
- <sup>45</sup>L. J. LeBlanc *et al.*, "Direct observation of zitterbewegung in a Bose-Einstein condensate," New J. Phys. 15 (2013).
- <sup>46</sup>W. Zhi-Yong and X. Cai-Dong, "Zitterbewegung in quantum field theory," Chin. Phys. B 17, 4170–4174 (2008).
- <sup>47</sup>M. Zahiri-Abyaneh and M. Farhoudi, "Zitterbewegung in External Magnetic Field: Classic versus Quantum Approach." Found. Phys. 41, 1355–1374 (2011).
- tum Approach," Found. Phys. 41, 1355–1374 (2011).

  48 J. G. Baixauli, "The Origin of Up and Down Quarks," SciFed Journal of Quantum Physics 3 (2019).
- <sup>49</sup>A. Buchmann and E. M. Henley, "Intrinsic quadrupole moment of the nucleon," Phys. Rev. C **63** (2001).
- <sup>50</sup>PHENIX Collaboration, "Creation of quark-gluon plasma droplets with three distinct geometries," Nature Physics 15, 214–220 (2019).
- <sup>51</sup>J. A. Miranda-Colón, "Heuristic solution to the conundrum of the zitterbewegung," Journal of Modern Physics 13, 301–314 (2022).
- <sup>52</sup>A. N. Lowan and G. Blanch, "Tables of Planck's Radiation and Photon Functions\*," J. Opt. Soc. Am. 30, 70–81 (1940).
- <sup>53</sup>M. Duncan, R. Myrzakulov, and D. Singleton, "Entropic derivation of F = ma for circular motion," Phys. Lett. B **703**, 516–518 (2011).
- <sup>54</sup>H. Ohanian, Spacetime and Gravitation, 1st ed. (Norton, New York, 1976) Chap. 8.
- <sup>55</sup>E. G. Haug, "Newton's and Einstein's Gravity in a New Perspective for Planck Masses and Smaller Sized Objects," Astron. Astrophys. 8, 6–23 (2018).
- <sup>56</sup>A. L. Peratt, *Physics of the Plasma Universe*, 2nd ed. (Springer, 2014).